

All-optical format conversions from NRZ to BPSK and QPSK based on nonlinear responses in silicon microring resonators

Yuanyuan Lu¹, Fangfei Liu¹, Min Qiu², and Yikai Su^{1*}

¹State Key Laboratory of Advanced Optical Communication Systems and Networks, Department of Electronic Engineering, Shanghai Jiao Tong University, Shanghai 200240, China

²Department of Microelectronics and Applied Physics, Royal Institute of Technology, Electrum 229, 16440, Kista, Sweden

*Corresponding author: yikaisu@sjtu.edu.cn

Abstract: We propose and numerically verify a novel scheme of all-optical format conversion from non-return-to-zero (NRZ) to binary phase-shift-keying (BPSK) at 160 Gb/s using cascaded microring resonators (CMRR) on a single silicon chip. The conversion is based on large phase shift and flattened intensity-response characteristics in the CMRR. A continuous-wave light experiences different phase shifts controlled by the power of an input NRZ signal with an ~8.8-dB extinction ratio, while maintaining approximately the constant intensity. All-optical format conversion from NRZ to quadrature phase-shift-keying (QPSK) is also demonstrated based on parallel NRZ/BPSK converters in a Mach-Zehnder interferometer structure.

©2007 Optical Society of America

OCIS codes: (060.5060) Phase modulation; (070.4340) Nonlinear optical signal processing; (060.4510) Optical communications; (230.1150) All-optical devices.

References and links

1. C. G. Lee, Y. J. Kim, Chul S. Park, H. J. Lee, and Chang -S. Park, "Experimental demonstration of 10-Gb/s data format conversion between NRZ and RZ using SOA-Loop-Mirror," *J. Lightwave Technol.* **23**, 834–841 (2005).
2. L. Xu, B. C. Wang, V. Baby, I. Glesk, and P. R. Prucnal, "All-optical data format conversion between RZ and NRZ based on a Mach-Zehnder interferometric wavelength converter," *IEEE Photon. Technol. Lett.* **15**, 308–310 (2003).
3. W. Li, M. Chen, Y. Dong, and S. Xie, "All-optical format conversion from NRZ to CSRZ and between RZ and CSRZ using SOA-based fiber loop mirror," *IEEE Photon. Technol. Lett.* **16**, 203–205 (2004).
4. J. Yu, G. K. Chang, J. Barry, and Y. Su, "40 Gbit/s signal format conversion from NRZ to RZ using a Mach-Zehnder delay interferometer," *Opt. Commun.* **248**, 419–422 (2005).
5. L. Zhou, H. Chen, and A.W. Poon, "NRZ-to-PRZ format conversion using silicon second-order coupled-microring resonator-based notch filters," in *Conference on Lasers and Electro-Optics* (Optical Society of America, 2007), paper CThP4.
6. T. Kawanishi, T. Sakamoto, and M. Izutsu, "All-optical modulation format conversion from frequency-shift-keying to phase-shift-keying," *Opt. Express* **13**, 8038–8044 (2005).
7. A. H. Gnauck, G. Raybon, S. Chandrasekhar, J. Leuthold, C. Doerr, L. Stulz, and E. Burrows, "25×40-Gb/s copolarized DPSK transmission over 12×100-km NZDF with 50-GHz channel spacing," *IEEE Photon. Technol. Lett.* **15**, 467–469 (2003).
8. T. Mizuochi, K. Ishida, T. Kobayashi, J. Abe, K. Kinjo, K. Motoshima, and K. Kasahara, "A comparative study of DPSK and OOK WDM transmission over transoceanic distances and their performance degradations due to nonlinear phase noise," *J. Lightwave Technol.* **21**, 1933–1943 (2003).
9. C. Yan, Y. Su, L. Yi, L. Feng, X. Tian, X. Xu, and Y. Tian, "All-optical format conversion from NRZ to BPSK using a single saturated SOA," *IEEE Photon. Technol. Lett.* **18**, 2368–2370 (2006).
10. K. Mishina, A. Maruta, S. Mitani, T. Miyahara, K. Ishida, K. Shimizu, T. Hatta, K. Motoshima, and K. Kitayama, "NRZ-OOK-to-RZ-BPSK modulation-format conversion using SOA-MZI wavelength converter," *J. Lightwave Technol.* **24**, 3751–3758 (2006).

11. C. S. Langhorst, R. Ludwig, M. Galili, B. Huettl, F. Futami, S. Watanabe, and C. Schubert, "160 Gbit/s all-optical OOK to DPSK in-line format conversion," in *Proceedings of the European Conference on Optical Communication (ECOC 2006)*, PD Th4.3.5.
12. S. H. Lee, K. K. Chow, C. Shu, and C. Lin, "All optical ASK to DPSK format conversion using cross-phase modulation in a nonlinear photonic crystal fiber," in *Conference on Lasers and Electro-Optics (2005)*, paper CFJ2-5.
13. K. Mishina, S. M. Nissanka, A. Maruta, S. Mitani, K. Ishida, K. Shimizu, T. Hatta, and K. Kitayama, "All-optical modulation format conversion from NRZ-OOK to RZ-QPSK using parallel SOA-MZI OOK/BPSK converters," *Opt. Express* **15**, 7774-7785 (2007).
14. H. M. van Driel, S. W. Leonard, H.-W. Tan, A. Birner, J. Schilling, S. L. Schweizer, R. B. Wehrspohn, and U. Gosele, "Tuning 2-D photonic crystals," *Proc. SPIE* **5511**, 1-9 (2004).
15. S. Blair, J. E. Heebner, and R. W. Boyd, "Beyond the absorption-limited nonlinear phase shift with microring resonators," *Opt. Lett.* **27**, 357-359 (2002).
16. V. Van, T. A. Ibrahim, P. P. Absil, F. G. Johnson, R. Grover, and P.-T. Ho, "Optical signal processing using nonlinear semiconductor microring resonators," *IEEE J. Sel. Top. Quantum Electron.* **8**, 705-713 (2002).
17. Y. Chen and S. Blair, "Nonlinear phase shift of cascaded microring resonators," *J. Opt. Soc. Am. B* **20**, 2125-2132 (2003).
18. J. E. Heebner and R. W. Boyd, "Enhanced all-optical switching by use of a nonlinear fiber ring resonator," *Opt. Lett.* **24**, 847-849 (1999).
19. L. Yin and G. P. Agrawal, "Impact of two-photon absorption on self-phase modulation in silicon waveguides," *Opt. Lett.* **32**, 2031-2033 (2007).
20. H. K. Tsang, C. S. Wong, T. K. Liang, I. E. Day, S. W. Roberts, A. Harpin, J. Drake, and M. Asghari, "Optical dispersion, two-photon absorption and self-phase modulation in silicon waveguides at 1.5 μ m wavelength," *App. Phys. Lett.* **80**, 416-418 (2002).
21. K. Croussore, C. Kim and G. Li, "All-optical regeneration of differential phase-shift keying signals based on phase-sensitive amplification," *Opt. Lett.* **28**, 2357-2359 (2004).

1. Introduction

All-optical modulation-format conversion may become a key technology for future optical networks, which could employ different modulation formats according to the network scales and applications. There have been various reports on format conversions between on-off-keying (OOK) signals [1-5], such as non-return-to-zero (NRZ), return-to-zero (RZ) and carrier-suppressed return-to-zero (CSRZ). Format conversion from frequency-shift-keying (FSK) to phase-shift-keying (PSK) was proposed based on optical double-sideband modulation technique [6]. While cost-effective OOK formats are widely employed in optical metro networks, PSK formats have been demonstrated advantageous over OOK for long-haul transmission systems [7, 8]. Therefore, all-optical format conversion from OOK to PSK would be desirable at gateway nodes between metropolitan area networks and wide area networks [9]. Format conversion from OOK to PSK can be realized using nonlinearity in semiconductor optical amplifiers (SOAs) [9, 10], cross-phase modulation (XPM) in highly nonlinear fiber (HNLF) [11], or XPM in photonic crystal fiber (PCF) [12]. Recently, conversion from OOK to QPSK has been proposed based on four integrated SOAs in a Mach-Zehnder interferometer (MZI) configuration [13]. However, the bit rates of the schemes based on SOAs are limited by their slow recovery time. The nonlinearity in HNLF or PCF is attractive in format conversion due to its ultrafast nonlinear response. However, a long interaction length is required in order to obtain sufficient nonlinear effects, which may limit the integration of the converters.

In this paper, we present a novel scheme for NRZ to binary phase-shift-keying (BPSK) format conversion by cascading microring resonators on a silicon chip. We also propose NRZ to quadrature phase-shift-keying (QPSK) format conversion using a parallel NRZ/BPSK converter. The conversion is based on the nonlinear-resonance detuning characteristics caused by Kerr effects in silicon, which is feasible at 160 Gb/s or even higher bit rates [14]. Silicon microring resonators, which exhibit much stronger nonlinearity than fibers [15], would be preferable to provide compact-device solutions in optical signal processing. An additional attractive feature of silicon converters is the opportunity to be compatible with the

mature CMOS fabrication process. In section 2, we present the principles of the NRZ to BPSK and NRZ to QPSK format conversions. The simulation results and conclusions are provided in section 3 and section 4, respectively.

2. Theory and operation principle

Figure 1(a) shows the schematic diagram of the proposed NRZ to BPSK format conversion. The converter consists of four cascaded microring resonators (CMRR) on a silicon chip. In fact, the number of resonators in CMRR can be varied depending on the parameters of the resonator and the extinction ratio of the input NRZ signal. An amplified NRZ signal at a wavelength λ_1 and a weak continuous-wave (CW) light at a wavelength λ_0 are coupled and launched into the CMRR simultaneously, as a pump and a probe light, respectively. Both λ_0 and λ_1 sit on resonances to maximize the powers coupled into the rings. The phase of the probe light propagating in the rings is changed due to the cross-phase modulation by the pump. This nonlinearly-induced single-pass phase shift detunes the probe light from the resonance of the cavity, thus causing a large effective transmission phase shift. Under proper operating conditions, after passing through the CMRR, the probe light experiences a phase shift of π when the pump is present (input of '1'), and a phase shift of 0 when the pump is absent (input of '0'). By properly adjusting the power of the pump pulse with finite extinction ratio, the amplitude of the probe light remains approximately constant at the output of the CMRR, because the amplitude change of the probe light with respect to the phase shift in the resonator is close to zero near resonance [16]. Thus, NRZ to BPSK is achieved through this process. The optical bandpass filter (BPF) blocks the NRZ signal at λ_1 , and only passes the converted BPSK signal at λ_0 . The converted BPSK signal can be demodulated by a Mach-Zehnder delay interferometer (MZDI) with 1-bit delay and received by a conventional balanced receiver. In practice, a post-decoding stage would be necessary to ensure the correct reception of the signal.

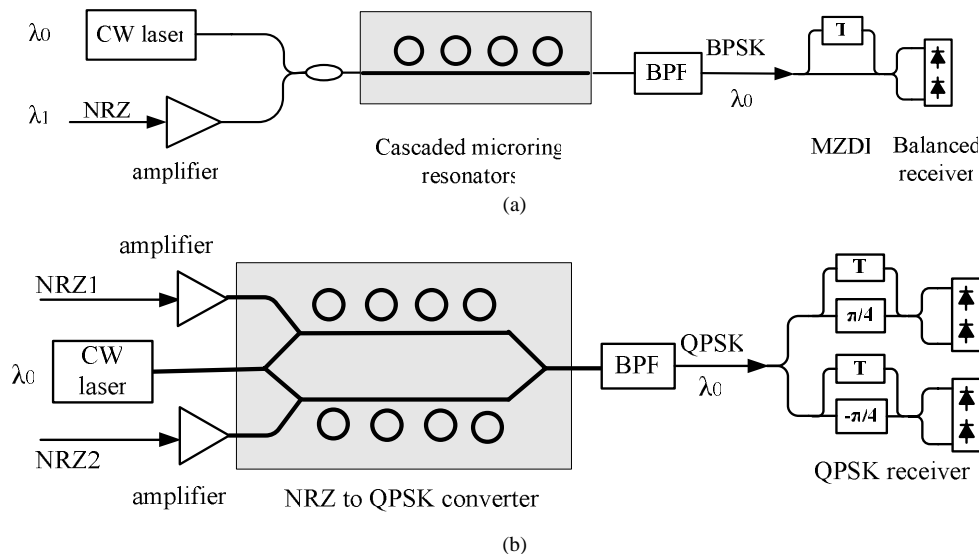


Fig. 1. Schematic diagrams of format conversions for (a) NRZ to BPSK and (b) NRZ to QPSK.

Similarly, Fig. 1(b) shows the schematic diagram of the proposed NRZ to QPSK format conversion. The converter consists of parallel CMRR-based NRZ to BPSK converters with a $\pi/2$ phase offset in a MZI configuration. The phase difference between the two arms in the MZI can be temperature-controlled. Two NRZ sequences are launched into the upper and lower arms of the MZI with the probe light, respectively. The probe light experiences a phase shift of 0 or π in the upper CMRR, and a phase shift of $-\pi/2$ or $\pi/2$ in the lower CMRR. After

orthogonal interference in the combiner of the MZI, the probe light will have four possible phases depending on the incoming NRZ signals, with almost flat amplitudes. In this manner, NRZ signals are converted into a QPSK signal. The QPSK signal can be demodulated using two MZDIs with a relative phase shift of $\pm\pi/4$ and detected by two balanced receivers.

We show the structure of a single microring resonator in Fig. 2(a), whose nonlinear response characteristics are plotted in Fig. 2(b) and will be studied in the following. The nonlinear response characteristics are general for any over-coupled microring resonator, although the required signal power may vary depending on the parameters of the microring resonator, such as its radius, width, coupling coefficient, and linear loss coefficient. By increasing the incident pump power, phase shift of the probe as much as π can be obtained. However, the intensity is modulated simultaneously, which is not desired for the NRZ to BPSK conversion. Compared with single microring resonator, CMRR can obtain more than π phase shift while maintaining constant intensity response [17], which is preferred for the conversion. Figure 2(c) illustrates the operation principle of the NRZ to BPSK format conversion in a CMRR with four rings. One can see that the pump produces a phase-shift difference of π on the probe light with approximately the constant amplitude through the CMRR. By properly adjusting the input power, the NRZ signal can be converted to the BPSK data. More flattened transmission response and larger nonlinear phase shift can be expected for more cascaded resonators in this configuration.

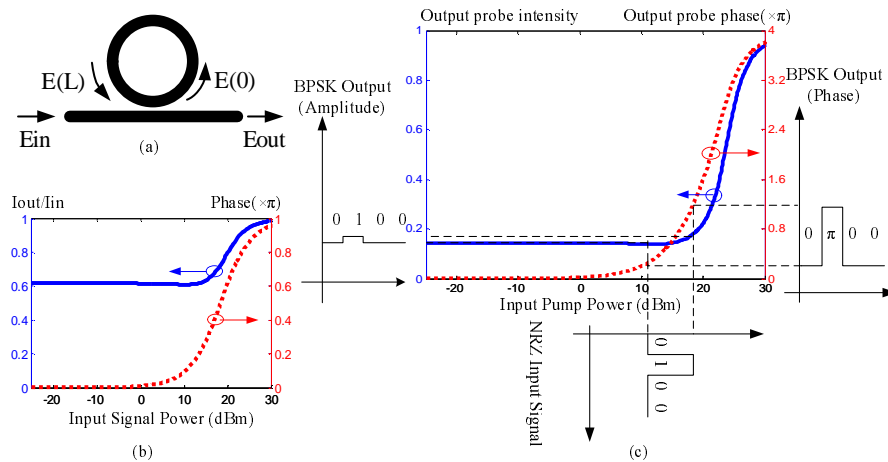


Fig. 2. (a) Structure of a single ring resonator. (b) Nonlinear response versus incident power in a single ring resonator: intensity transmittance (solid) and output phase shift (dashed). (c) Operation principle of NRZ to BPSK format conversion in CMRR.

Here we explain the principle of the CMRR in the format conversion process. When the high-intensity pump and the weak probe light propagate in the CMRR, there are four major nonlinear effects, including self-phase modulation (SPM), degenerate two-photon absorption (TPA) on the pump signal, cross-phase modulation (XPM), and non-degenerate TPA on the probe light. The processes of SPM and degenerate TPA in CMRR have been extensively studied [15, 17]. In the following, we concentrate on the processes of XPM and non-degenerate TPA in CMRR and assume that the probe light is much weaker than the pump pulses.

We begin with the fundamental mechanism in a single microring resonator. The coupler is modeled as a directional coupler [18], obeying the field transfer characteristics described by

$$\begin{bmatrix} E_{out} \\ E(0) \end{bmatrix} = \begin{bmatrix} \tau & i\sigma \\ i\sigma & \tau \end{bmatrix} \begin{bmatrix} E_{in} \\ E(L) \end{bmatrix}, \quad (1)$$

where $E(0)$ and $E(L)$ are the field amplitudes in the resonator, E_{in} and E_{out} are the input and output field amplitudes, respectively, and the coupling (σ) and transmission (τ) coefficients are related by $\sigma^2 + \tau^2 = 1$. $E(0)$ and $E(L)$ are related by

$$E(L) = a \exp(+i\phi)E(0), \quad (2)$$

where L is the circumference of the ring, a is the field attenuation including both linear absorption and two-photon absorption (TPA), and ϕ is the single-pass phase shift in one ring including the linear phase shift in propagation and nonlinear phase shift due to the Kerr effect and TPA loss. In our simulations, each ring is assumed to have the same radius $R = 9\mu\text{m}$, linear attenuation coefficient $\alpha = 2/\text{cm}$, and coupling coefficient $\sigma = 0.3$.

By solving Eq. (1), we have:

$$\frac{E_{out}}{E_{in}} = \frac{\tau - a \exp(+i\phi)}{1 - \tau a \exp(+i\phi)}. \quad (3)$$

The total transmission phase-shift of the output field (E_{out}) is

$$\Delta\Phi = \arctan \frac{\tau a \sin(\phi)}{1 - \tau a \cos(\phi)} - \arctan \frac{a \sin(\phi)}{\tau - a \cos(\phi)}, \quad (4)$$

which is largely dependent on the single-pass phase shift near resonance.

One can obtain the following propagation equation from nonlinear Schrödinger (NLS) equation, which describes the change in amplitude of the probe light as a function of distance:

$$\frac{\partial E_0}{\partial z} + \frac{\alpha}{2} E_0 + \frac{\beta_{non-deg}}{2} (2|E_1|^2) E_0 = i \frac{n_2 \omega_0}{c} (2|E_1|^2) E_0, \quad (5)$$

where E_0 and E_1 are the complex amplitudes of the probe light and the pump pulse, respectively, ω_0 is the frequency of the probe light, n_2 is the nonlinear Kerr index, and $\beta_{non-deg}$ is the non-degenerate TPA coefficient, which is a little different from degenerate TPA coefficient. However, the difference can be neglected in practice. In Eq. (5), we ignore the material dispersion which will be included in the total phase shift in the following.

Substituting $E = \sqrt{I} \exp(i\phi_{NL} - \alpha z/2)$ in Eq. (5) and equating the real and imaginary parts [19], we obtain a differential equation for the intensity I_0 and one for the nonlinear phase ϕ_{NL} :

$$\frac{\partial I_0}{\partial z} = -\beta_{non-deg} (2I_1) I_0 \exp(-\alpha z), \quad (6a)$$

$$\frac{\partial \phi_{NL}}{\partial z} = \frac{n_2 \omega_0}{c} (2I_1) \exp(-\alpha z). \quad (6b)$$

where I_0 and I_1 are the intensity of the probe light and the pump pulse, respectively. As the TPA effect on the intensity of the pump and the probe light is about 4 orders of magnitude less than the linear attenuation, we can assume that I_1 varies in proportional to I_0 along a short length L , i.e., $I_1(z) = mI_0(z)$, where m is a constant. By solving Eq. (6), one can have:

$$I_0(L) = \frac{I_0(0)\exp(-\alpha L)}{1 + 2\beta_{\text{non-deg}} I_1(0)L_{\text{eff}}}, \quad (7a)$$

$$\phi_{NL} = \frac{n_2\omega_0}{c\beta_{\text{non-deg}}} \ln(1 + 2\beta_{\text{non-deg}} I_1(0)L_{\text{eff}}), \quad (7b)$$

where $I_1(0)$ is the incident intensity of the pump pulse in the ring at the coupler, and $L_{\text{eff}} = [1 - \exp(-\alpha L)]/\alpha$ is the effective interaction length due to the linear absorption. Substituting Eq. (2) in Eq. (7a), and including the linear phase shift into the total phase shift ϕ , we obtain

$$a^2 = \frac{\exp(-\alpha L)}{1 + 2\beta_{\text{non-deg}} I_1(0)L_{\text{eff}}}, \quad (8a)$$

$$\phi = k_0 L + \frac{n_2\omega_0}{c\beta_{\text{non-deg}}} \ln(1 + 2\beta_{\text{non-deg}} I_1(0)L_{\text{eff}}), \quad (8b)$$

where $k_0 = 2\pi n(\omega_0)/\lambda_0$ is the linear phase constant of the probe light.

Substituting Eq. (8) into Eq. (3) and Eq. (4) gives the nonlinear transmission response in the presence of XPM and non-degenerate TPA. Figure 2(b) shows the simulated nonlinear intensity and phase responses of the probe light in a single microring resonator, with $n_2 = 6 \times 10^{-18} \text{ m}^2/\text{W}$ and $\beta_{\text{non-deg}} = 0.45 \text{ cm}/\text{GW}$ [20]. By cascading the four microring resonators in sequence, we obtain the nonlinear intensity and phase responses of the probe light at resonance in the CMRR, as shown in Fig. 2(c). In this configuration, there is no coupling between the microrings in the horizontal direction, which are spaced by 2 μm . The total length of the strip waveguide in the CMRR is less than 100 μm , thus the propagation loss can be neglected to simplify the simulation.

3. Simulation results and discussion

Figure 3 provides the simulation results of the NRZ to BPSK format conversion. The input NRZ signal is a 2^9-1 pseudorandom binary sequence (PRBS) at 160 Gb/s with an ~ 8.8 -dB extinction ratio, whose waveform, eye diagram, and spectrum are shown in Fig. 3(a), (c), and (e), respectively. The data rate is limited by the response time of Kerr effect, which is on the order of femtosecond. Here we take 160 Gb/s for example to explain the operation principle of the converter. The wavelengths of the NRZ signal (1534.8nm) and the probe light (1545.2nm) are sitting at two different resonances. The peak power of the amplified NRZ signal is about 15.9 dBm. We assume that the input signal power is stabilized after it passes the amplifier. After passing through the CMRR, the weak probe light with a power of 0 dBm is converted into BPSK, whose phase, phase eye diagram, and spectrum are presented in Fig. 3(b), (d), and (f), respectively. The waveform and the amplitude eye diagram of the converted BPSK are provided in Fig. 3(g) and (h), respectively. The BPSK signal shows clear and open eyes in phase. The residual amplitude fluctuations on the BPSK signal are not expected to result in significant signal degradation through the filtering of the MZDI. In addition, phase-sensitive amplification for BPSK signal regeneration can be employed to suppress the amplitude fluctuation while retaining the phase information [21]. Figure 3(i) and (j) present the electric waveform and the eye diagram of the demodulated signal at the balanced receiver.

The proposed scheme is feasible for conversions of NRZ signals with varied extinction ratios by adjusting the input power of the pump or changing the number of the cascaded microrings. For low extinction ratios (< 8.8 dB), higher pump power or more microrings are needed to obtain an output phase shift of π with a constant intensity. The full-width at half depth (FWHD) of the CMRR is about 40 GHz. In our simulations, the CMRR is over-

coupled, and its transmission dip is very shallow, about 4-dB attenuation at the minimum, causing insignificant ripples on the NRZ pump signal.

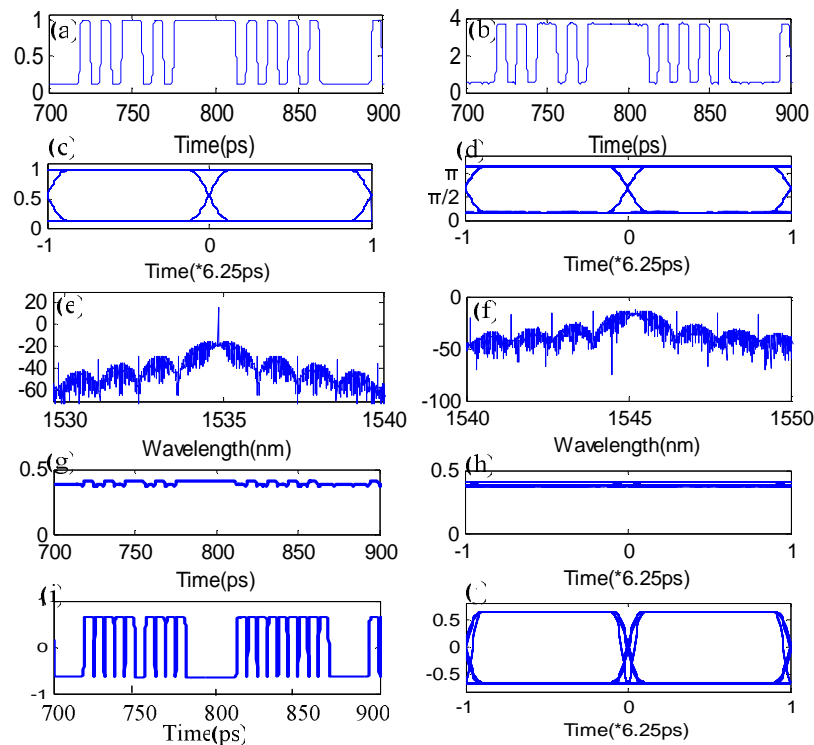


Fig. 3. Simulation results of NRZ to BPSK format conversion. (a), (c), (e) Amplitude, eye diagram, and spectrum of the input NRZ signal. (b), (d), (f) Phase, phase eye diagram, and spectrum of the output BPSK data. (g), (h) Amplitude and signal eye diagram of the BPSK data. (i), (j) Waveform and eye diagram of the demodulated signal.

Figure 4 provides the simulation results of the format conversion from NRZ to QPSK. Two branches of converted BPSK signals interfere orthogonally in the combiner of the MZI, and an optical QPSK signal can be obtained. The phase eye diagram and the optical spectrum of the converted QPSK data are shown in Fig. 4(a) and (b), respectively. Figure 4(c) and (d) show the eye diagrams of the demodulated QPSK signal at two balanced receivers. The overshoot and undershoot are caused by the interference between the two arms of the converted BPSK signals, which does not affect the decision at the center of each pulse.

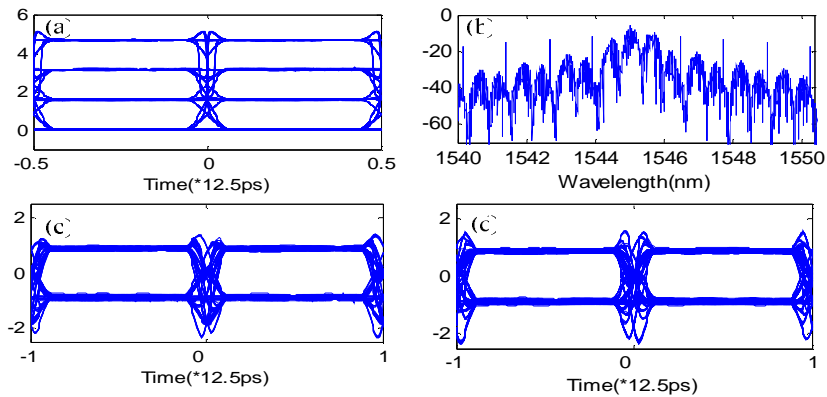


Fig. 4. Simulation results of NRZ to QPSK format conversion. (a) Phase eye diagram of the converted QPSK, (b) Optical spectrum of the converted QPSK. (c), (d) Eye diagrams of the in-phase and quadrature branches of the demodulated QPSK.

4. Conclusion

In conclusion, we have proposed and demonstrated, through simulations, a novel all-optical format conversion from NRZ to BPSK using CMRR on a silicon chip. This conversion scheme is advantageous due to the small size, high speed, low cost and integration features. NRZ to QPSK format conversion can be obtained using parallel CMRR-based NRZ/BPSK converters on a silicon chip. The schemes proposed in this paper may play an important role at intermediate nodes between metro networks and long-haul backbone networks.

Acknowledgments

This work was supported by the National Natural Science Foundation of China (60407008), the 863 High-Tech Program (2006AA01Z255), the key project of Ministry of Education (106071), the Shanghai Rising Star Program Phase II (07QH14008), and the Fok Ying Tung Fund (101067).